

Electronic and magnetic order as a function of doping in mixed-valent $\text{La}_{1-x}\text{Sr}_x\text{MnO}_3$ thin films

James Payne, Dakota Brown, Calleigh Brannan, Tom Pekarek, Maitri P. Warusawithana
Department of Physics, University of North Florida

Molecular Beam Epitaxy

- Our samples were grown using a technique known as Molecular Beam Epitaxy (MBE).
- In MBE, we utilize carefully calibrated molecular beams of constituent elements to produce thin films one atomic layer at a time
- Sources of the constituent elements are heated in effusion cells to evaporate material into the chamber, forming molecular beams.
- In oxide MBE, a form of oxygen is introduced into the chamber to form oxides.
- For our growths of $\text{La}_{1-x}\text{Sr}_x\text{MnO}_3$, ozone was employed as our source of oxygen, allowing us to keep the chamber pressure low (5E-7 Torr) due to ozone's high oxidizing potential.

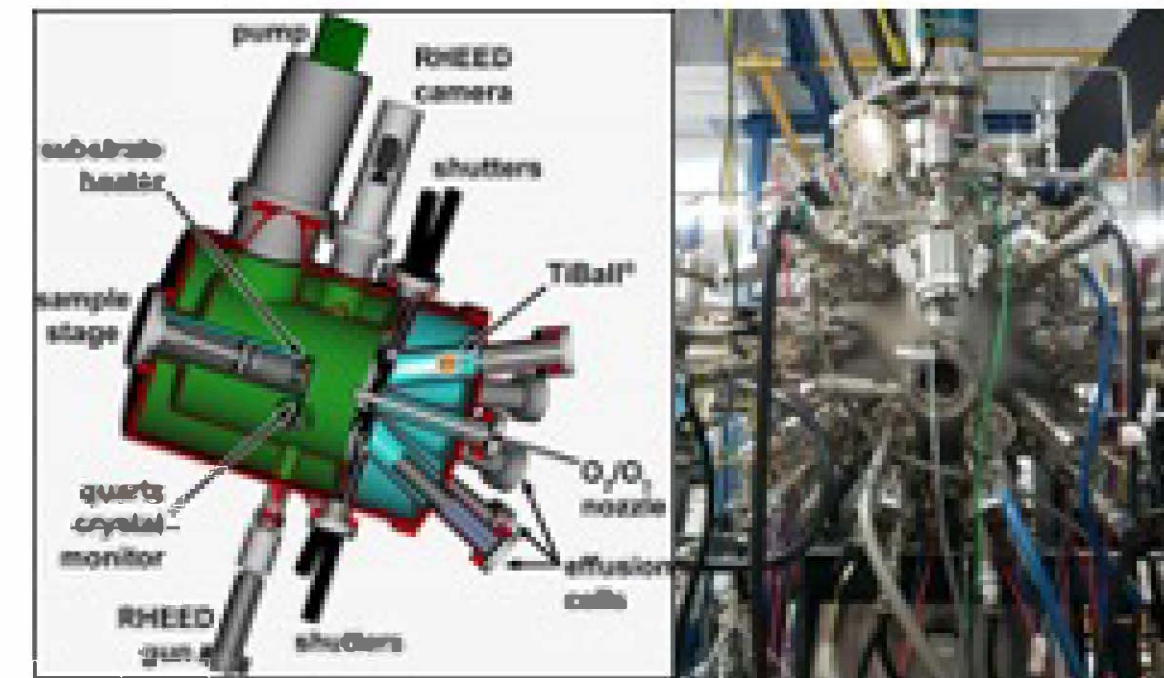


Fig. 1 (Left) A side view diagram of an MBE chamber. (Right) A front view picture of the chamber used in our growths.

Bulk Phase Behavior

- The behavior of $\text{La}_{1-x}\text{Sr}_x\text{MnO}_3$ has been extensively documented in bulk crystals with respect to temperature and strontium concentration.
- Undoped LaMnO_3 is known to be a Mott insulator that at higher temperatures has paramagnetic behavior and becomes antiferromagnetic at lower temperatures.
- In the range around $x=0.4$ $\text{La}_{1-x}\text{Sr}_x\text{MnO}_3$ is a paramagnetic insulator at higher temperatures but at lower temperatures it transitions to a ferromagnetic conductor.
- This ferromagnetic-conducting state is kinetically favorable around $x=0.4$ at lower temperatures because the double exchange interaction allows for the delocalization of electrons across spin aligned manganese atoms, reducing free energy.

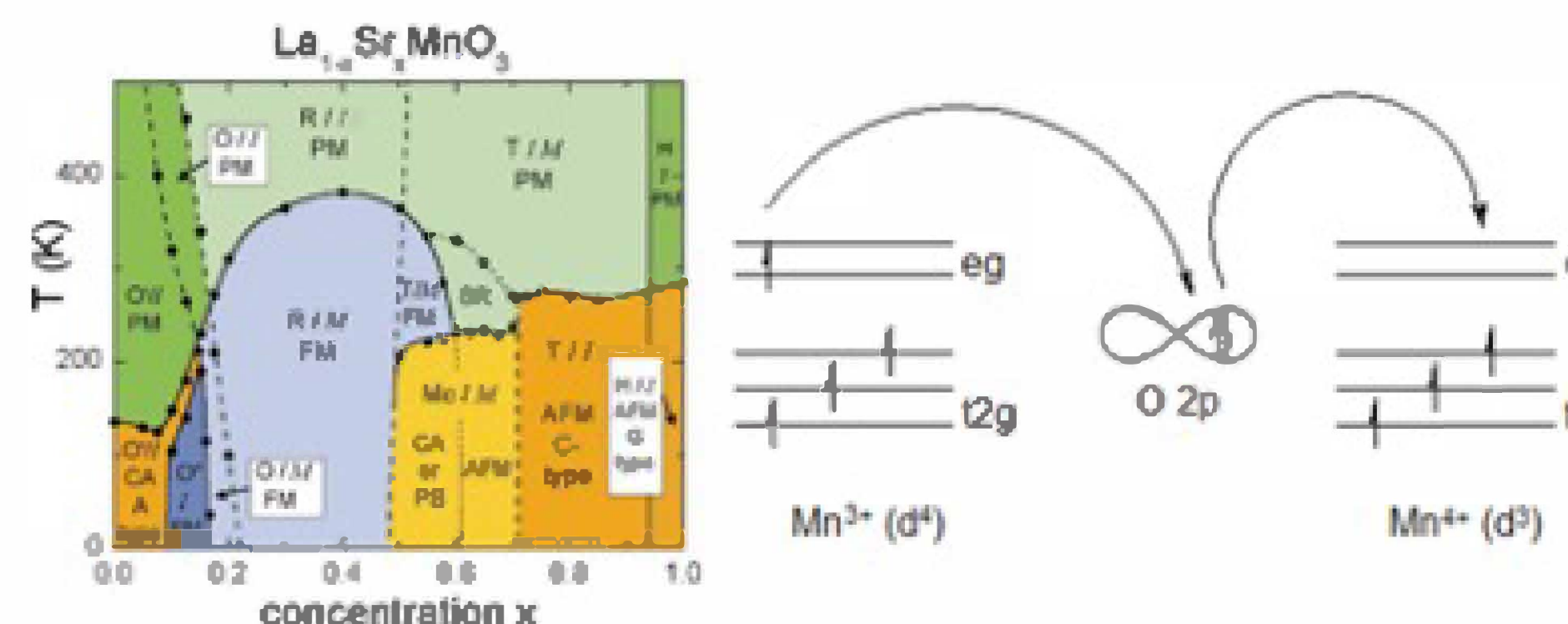


Fig. 3 (Top) The phase diagram of $\text{La}_{1-x}\text{Sr}_x\text{MnO}_3$ in bulk.¹ (Bottom) Mechanism for the double exchange interaction.

Thin Films of $\text{La}_{1-x}\text{Sr}_x\text{MnO}_3$ for Different Doping Concentrations

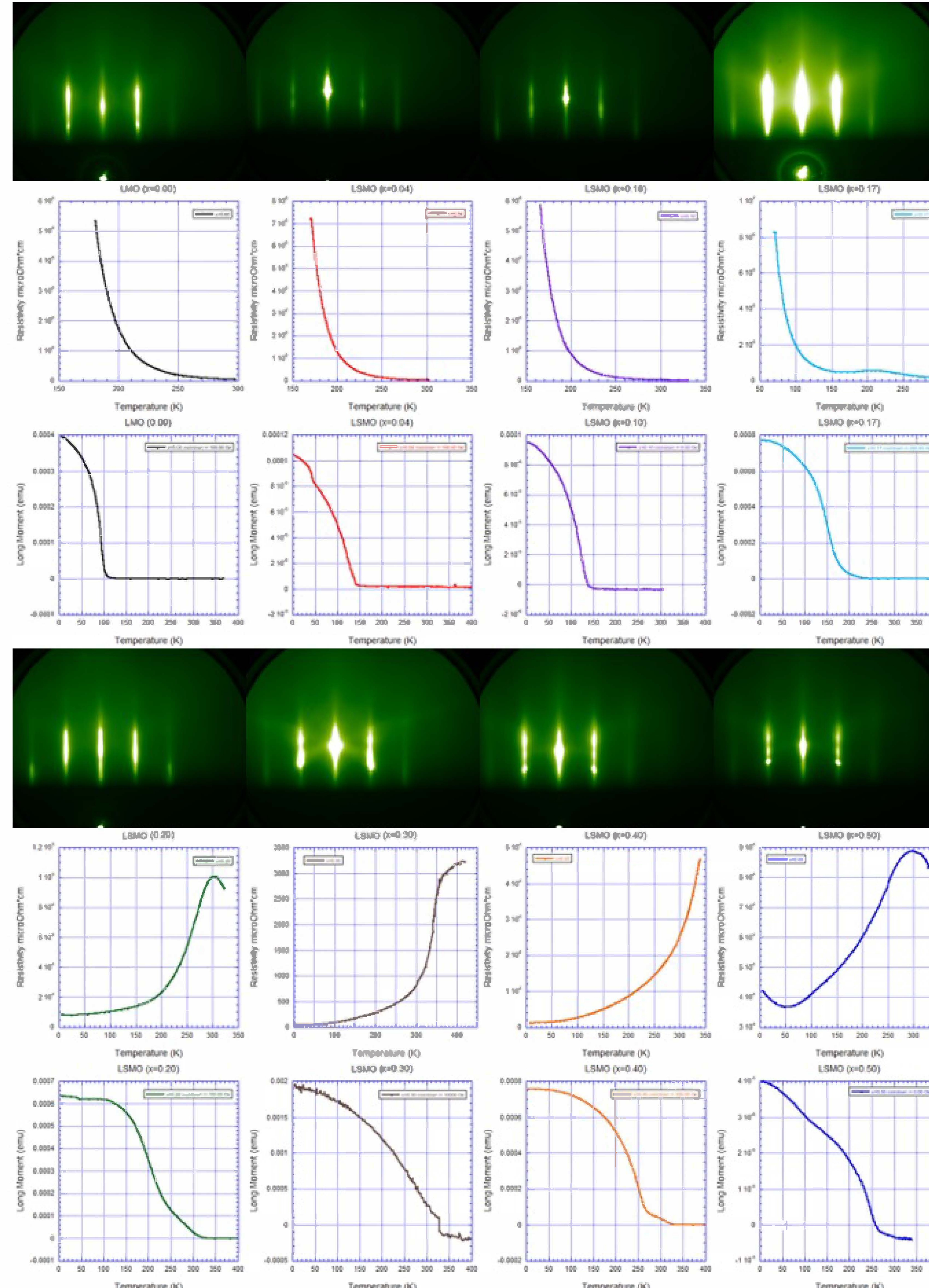


Fig. 5 (Top) Reflection high energy electron diffraction (RHEED) patterns taken during the growth of each sample ($x=0, 0.04, 0.10, 0.17, 0.20, 0.30, 0.40, 0.50$). (Middle) The measure of film resistivity as a function of temperature for each sample. (Bottom) The measure of film magnetic field, collected in a field cooldown, as a function of temperature for each sample.

- An atomic force microscopy scan was done for the $x=0.30$ film. In this scan, figure 4, terraces can be seen in the surface morphology, which is indicative that the film is flat and strained to the substrate.
- Additionally, Reflection high energy electron diffraction (RHEED) patterns taken near the end of the growths, shown in figure 5, also indicate well-strained growth and a 2-dimensional surface morphology.
- From the film transport and magnetic data, figure 5 and 6, we can observe transitions in the electronic and magnetic ordering of the samples.
- Samples $x=0, 0.04$, and 0.10 are shown to be insulators over the entire temperature range measured, with magnetic ordering in the $x=0$ sample below around 100K and below 140K for the $x=0.04$ and 0.10 samples.
- In $x=0.20, 0.30$, and 0.40 we observe a ground state conducting behavior, while insulating behavior is present below 50K in $x=0.50$ and 170K in $x=0.17$
- A metal-to-insulator transition accompanied by magnetic ordering is observed below around: 210K for $x=0.17$, 310K for $x=0.20$, 400K for $x=0.30$, and 260K for $x=0.50$. We also observe magnetic ordering in $x=0.4$ below around 320K though no metal-to-insulator transition is observed within the measured range.

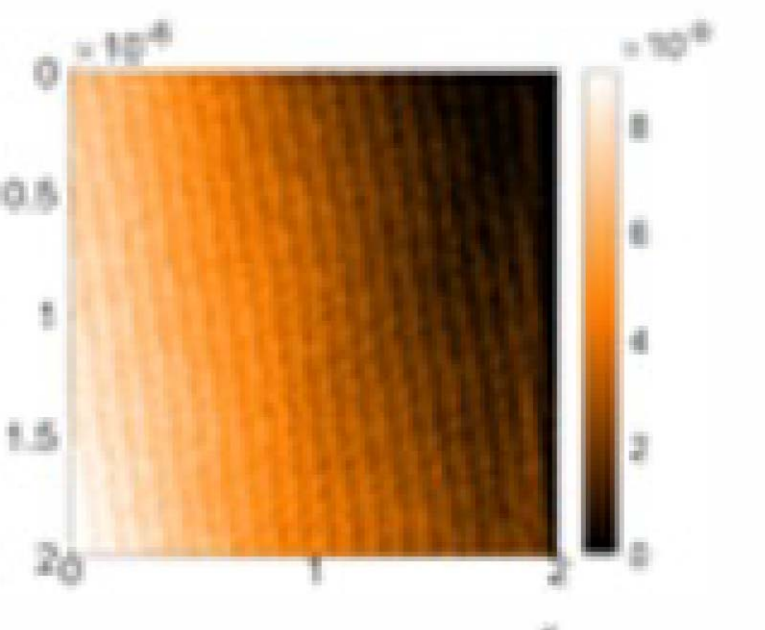


Fig. 4 Atomic force microscopy (AFM) image of the surface of the $x=0.3$ sample.

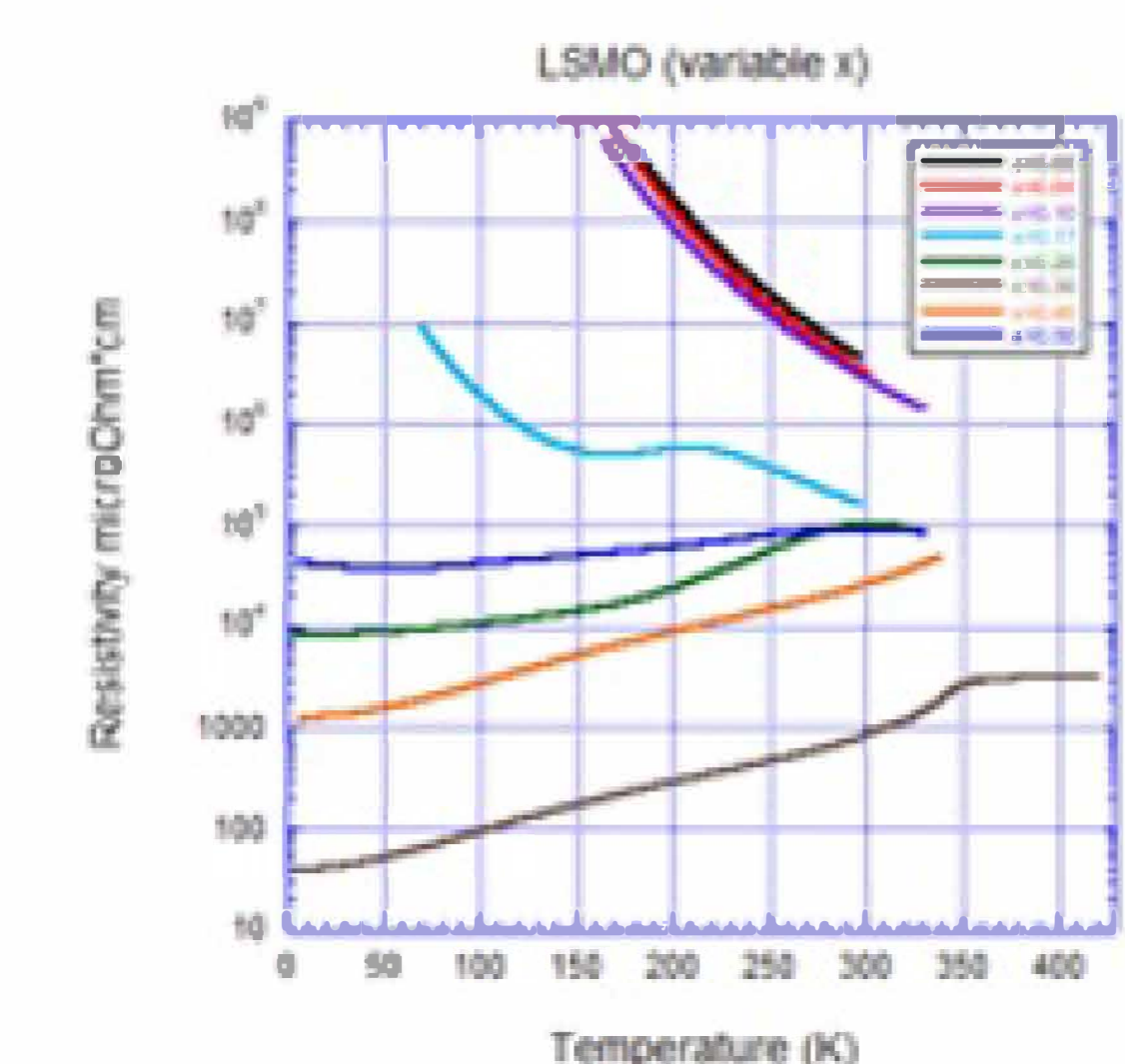


Fig. 6 Film resistivity as a function of temperature for $x=0, 0.04, 0.10, 0.17, 0.20, 0.30, 0.40$ and 0.50 compared on a log scale.

Reference